Progress In Electromagnetics Research C, Vol. 104, 129–141, 2020

Half U-Slot and Rectangular Slot Loaded Nearly Square Microstrip Antennas for Wideband Response

Venkata A. P. Chavali[1, *] and Amit A. Deshmukh[2]

Abstract—Wideband designs of nearly square microstrip antenna using two half U-slots and rectangular slots are proposed. The slots optimize the spacing in between the patch modified TM_{11}, TM_{20}, TM_{02}, and TM_{30} resonant modes to yield wideband response. The design with two half U-slots yields bandwidth of around 1000 MHz ($\sim 50\%$) whereas that with an additional rectangular slot yields bandwidth of 1345 MHz ($\sim 61\%$). Due to the presence of higher order modes, the proposed design offers higher cross polar radiation pattern across the entire bandwidth with the gain greater than 5 dBi. The formulations for the modified patch modes and subsequent redesign procedure are presented, which serve as a guideline in the designing of similar antennas around specific resonance frequency. With the given antenna characteristics, the proposed antennas will find applications in personal and mobile communication systems.

1. INTRODUCTION

An enhancement in the bandwidth (BW) of microstrip antenna (MSA) using a slot is a widely reported technique ever since the same was introduced in 1995 [1–3]. The slot introduces additional resonant mode near the fundamental patch mode that widens the impedance BW. Different slot shapes like U-shape, V-shape, rectangular shape, etc. and their modified variations have been reported to widen the BW [1–11]. A detailed study to explain the functioning of slot cut wideband antennas in terms of modified patch modes is reported [12, 13]. It showed that widening of the BW with the same polarization of the radiated field is a result of the optimization of frequency, impedance, and current variations at orthogonal higher order resonant modes with respect to the patch's fundamental mode. This study revealed that the placement of slot in the patch governs which higher order mode will contribute to BW enhancement. In personal and mobile communication systems, to minimize the signal loss because of the multi-path propagation, antennas which receive signal from any direction are preferred. Here either circularly polarized antennas or antennas which offer higher cross polar component (elliptical polarization) will be preferred. Realization of circularly polarized response needs the condition of time and space orthogonality of the patch modes to be satisfied over range of frequencies, and thus it is relatively complex to design. In the case of elliptical polarization, i.e., antenna offering higher cross polar level, the difference between the co- and cross-polar levels is around 5 to 10 dB, and thus they will also lead to minimum signal loss wideband MSAs obtained using slots offering lower cross-polar radiation over most of the impedance BW due to the unidirectional currents realized by the slot at fundamental and higher order orthogonal modes. Therefore, to realize a wideband MSA with higher cross polar component, slot cut antennas resonating around the fundamental patch mode cannot be used.

This paper presents the designs of nearly square MSA (SMSA) embedded with two half U-slots and rectangular slots for achieving wideband response offering higher cross-polar radiation pattern across

Received 2 June 2020, Accepted 16 July 2020, Scheduled 4 August 2020
* Corresponding author: Venkata A. P. Chavali (cpriyag@gmail.com).
[1] EXTC Department, SVKM's DJSCE, Mumbai, India. [2] EXTC Department, SVKM's DJSCE, Mumbai, India.

the impedance BW. Initially, the proposed configurations are discussed in 2000 MHz frequency band on a thicker air substrate (greater than $0.08\lambda_0$). In every configuration, a detailed study to explain the effects of slots on patch resonant modes is presented. Initially, two half U-slots optimize the spacing in between modified TM_{11} and TM_{20} modes of the patch to give impedance BW around 1000 MHz ($\sim 50\%$). The antenna offers a broadside pattern with a gain above 5 dBi across most of the BW. Further with the addition of a rectangular slot in half U-slots cut SMSA frequency of the next higher order TM_{02} mode is tuned with respect to TM_{11} and TM_{20} modes, to give a BW around 1254 MHz ($\sim 57\%$). This configuration also shows a broadside pattern with a gain above 5 dBi across the complete BW. Due to the presence of higher order modes, the proposed slot cut designs show a higher cross-polar radiation pattern across the entire BW. The resonant length formulations at modified fundamental (TM_{10}, TM_{01}) as well as higher order (TM_{11}, TM_{20}, TM_{02}) modes are presented. The frequencies calculated using them agree closely with simulated frequencies. Using the proposed formulations, the procedure to design similar configurations on air as well as suspended FR4 substrate ($\varepsilon_r = 4.3$, $h = 0.16$ cm) is presented, which gives a similar wideband response. Many configurations using slots have been reported in the literature. However, all those designs give BW around the fundamental mode frequency of the patch to yield a pattern with low cross-polar content. Hence, they will not be useful in personal and mobile communication applications. As against the reported slot cut antennas, the proposed configurations realize wideband response around the higher order mode frequencies of the patch thereby showing a pattern with higher cross polar content. , they will find their usage in above mentioned applications. Also design methodology using proposed formulations is explained in this paper, which is rarely explained in the reported papers for slot cut wideband designs. The detailed comparison for the proposed designs against some of the reported variations is provided in Table 2. Thus, the designs of multiple slots cut SMSAs offering impedance BW above 50% around the higher order resonant modes showing higher cross polar radiation pattern supported with detailed explanations and design methodology are the new technical contributions in the proposed work. The antennas studied in this paper are first optimized using CST software [20] followed by the experimentation using high frequency instruments namely, ZVH-8, FSC 6, and SMB 100 A.

2. TWO HALF U-SLOTS CUT SMSA

The design of a double U-slot cut rectangular MSA (RMSA) is shown in Fig. 1(a) [14]. This antenna yields the BW of 700 MHz (44%) on a substrate of thickness 1.65 cm ($0.09\lambda_g$) [4]. Here the impedance BW lies around the fundamental TM_{10} mode frequency of the RMSA shows a lower cross-polar radiation

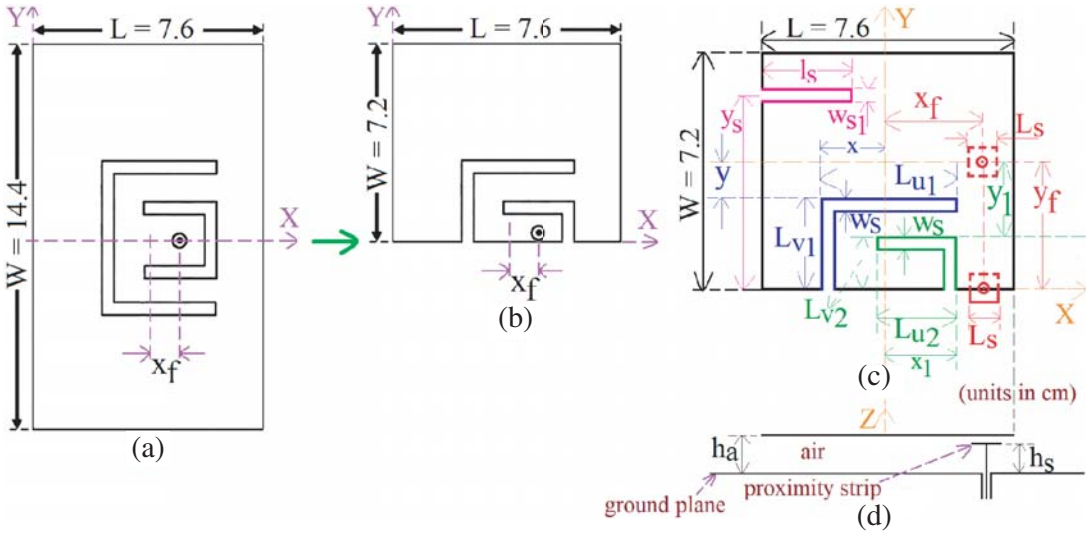

Figure 1. (a) Two U-slot cut RMSA, (b) two half U-slot cut nearly SMSA, (c), (d) proximity fed nearly SMSA embedded with two half U-slots and a rectangular slot.

pattern as two U-slots are symmetrically placed with respect to the patch center [14]. To realize a high cross-polar pattern, along with the excitation of higher order modes, surface current vectors on the patch are needed to be bidirectional. To achieve this, first the symmetry of two U-slot cut design is considered along the coaxial feed axis to realize nearly SMSA design embedded with two half U-slots. Here, the feed is placed on the patch edge as shown in Fig. 1(b). Further to realize a larger BW, proximity feeding is selected, and the patch is suspended in air using substrate thickness of 'h_a' = 2.0 cm as given in Figs. 1(c), (d).

Initially to optimize the wideband response parametric variations are carried out, and resonance curve plots for the increment in slot dimensions 'L_{v1}' and 'L_{u1}' are shown in Figs. 2(a) and (b). As the patch length and width are nearly the same, separate peaks due to TM_{10} and TM_{01} modes are not observed. Because of the offset feed, TM_{11} mode is present. With increase in vertical U-slot length 'L_{v1}', TM_{10} and TM_{11} mode frequencies decrease, as their modal currents are orthogonal to 'L_{v1}'. The TM_{20} mode frequency also decreases as the placement of 'L_{v1}' is near its maximum current location. Further with increase in 'L_{u1}' frequencies of all the resonant modes decrease. For 'L_{v1}' = 2.2 and 'L_{u1}' = 4.8 cm, the loop due to modified TM_{11} mode is optimized inside VSWR = 2 circle as shown in Fig. 2(c). Here the frequency of TM_{10} mode lies much below TM_{11} mode frequency, and thus it does not

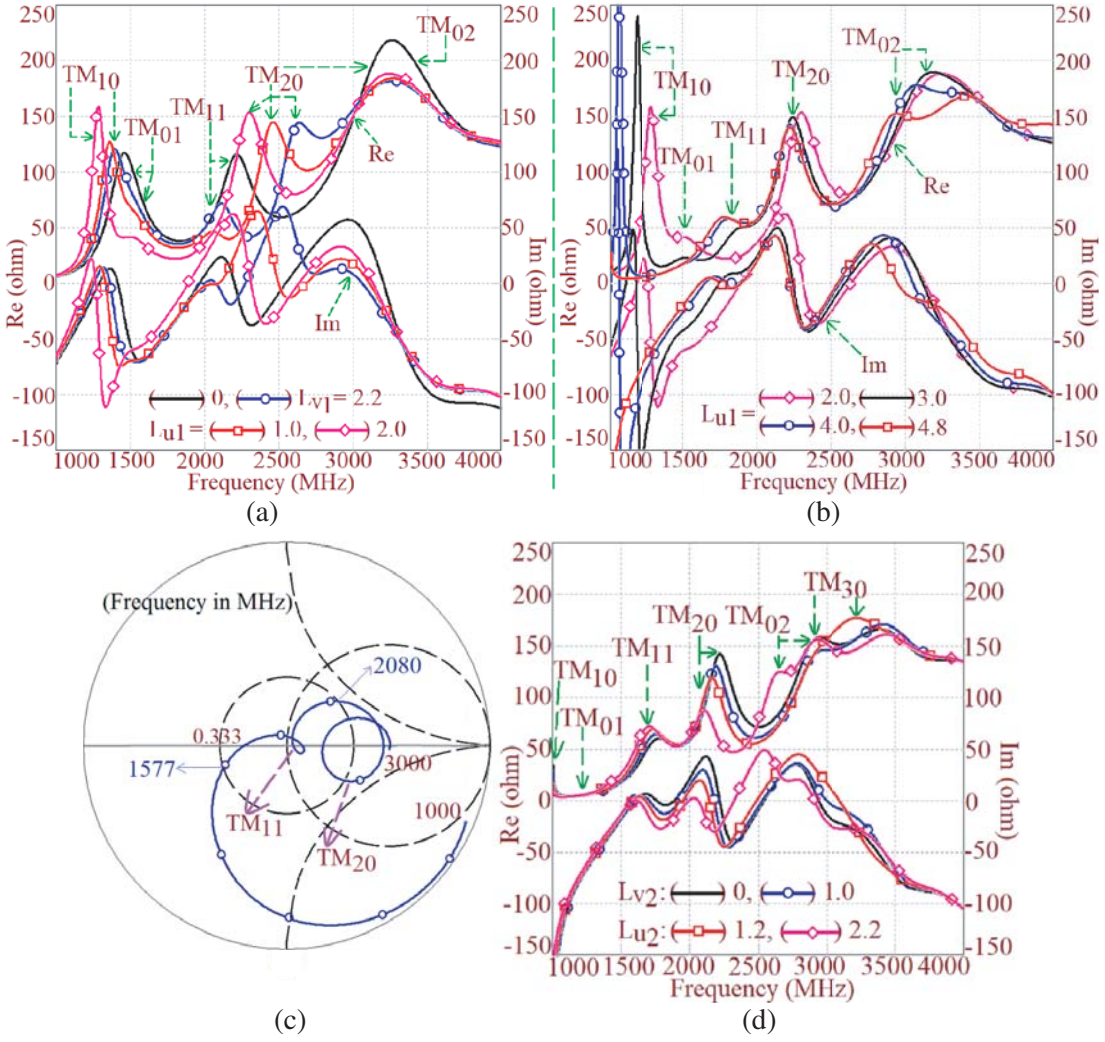

Figure 2. (a), (b) Resonance curve plots for increase in dimensions 'L_{u1}' and 'L_{v1}' of larger U-slot, (c) smith chart for half U-slot cut SMSA for 'L_{u1}' = 4.8 cm, 'h_s' = 1.8 cm and (d) resonance curve plot for increase in 'L_{v2}' and 'L_{u2}' of smaller half U-slot dimension.

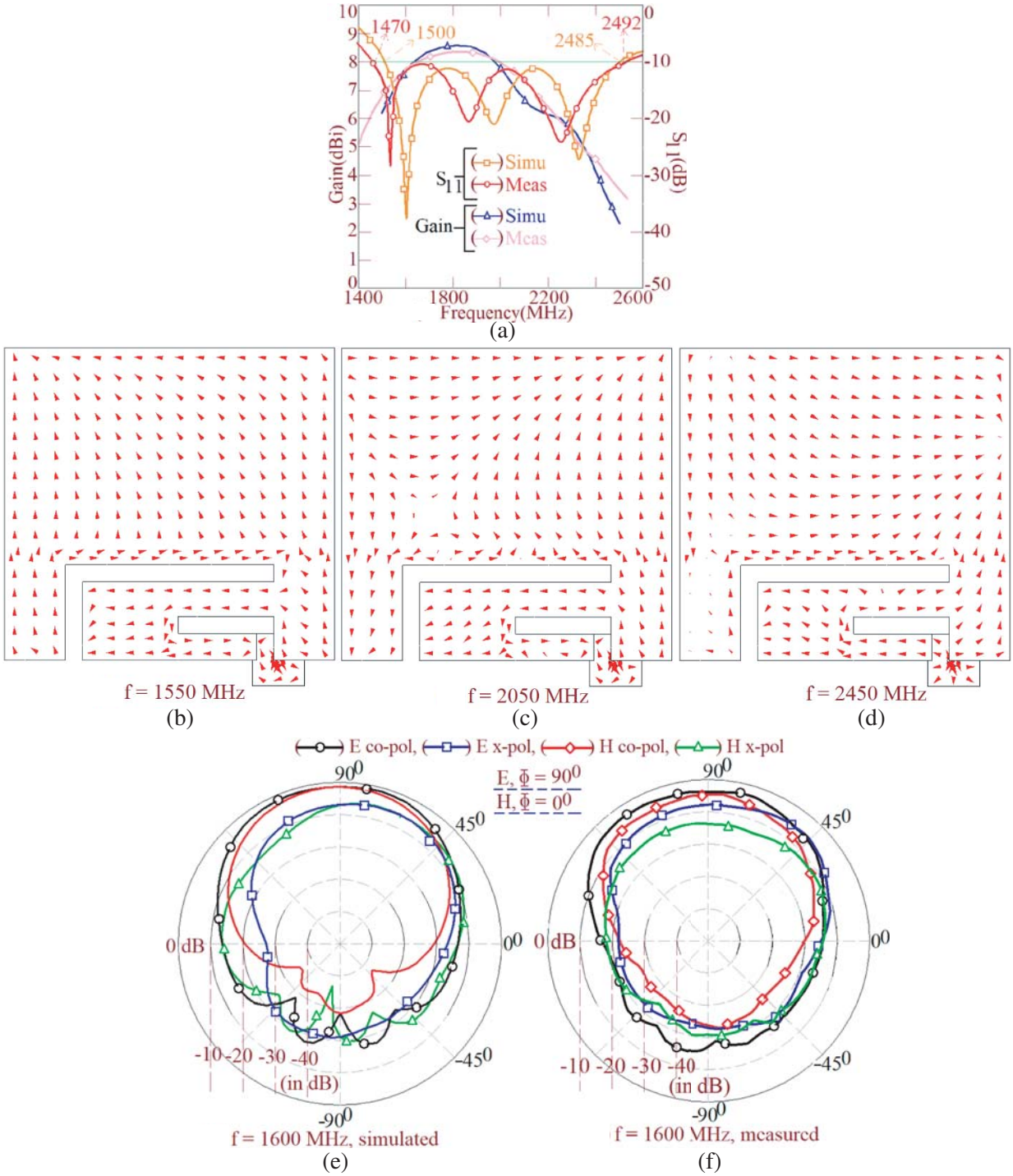

Figure 3. (a) Return loss plots, (b)–(d) surface current distributions at three frequencies across the BW and (e), (f) radiation pattern nearer to the band start frequency for SMSA with two half U-slots.

lie inside VSWR = 2 circle to contribute to the BW. With single half U-slot, simulated BW is 503 MHz (27.51%). The next loop observed in the Smith chart is due to modified TM_{20} mode. To increase the BW, the position of this loop can be optimized by embedding the second half U-slot of dimension 'L_{v2}' and 'L_{u2}', as shown in Fig. 1(c). The resonance curve plot for the second half U-slot length variation is shown in Fig. 2(d).

The increase in 'L_{v2}' and 'L_{u2}' reduces the frequency and impedance at TM_{20} mode due to which loop formed due to the same is optimized inside VSWR = 2 circle to give the maximum BW. The same is realized for 'L_{v2}' = 1.0 'L_{u2}' = 2.2, 'w_s' = 0.4, 'x_f' = 2.5, and 'y_f' = 0 cm, and return loss (S_{11}) plots for the optimum design are shown in Fig. 3(a). The simulated and measured BWs are 985 MHz (49.44%) and 1022 MHz 51.6%), respectively. The antenna gain is larger than 5 dBi over most of the BW with peak gain close to 9 dBi as shown in Fig. 3(a). Simulated surface current distributions at three frequencies over the BW and radiation pattern near the band stop and start frequencies are shown in Figs. 3(b)–(f) and 4(a), (b).

Due to the presence of modified TM_{11} and TM_{20} modes, current variation is bidirectional over the patch. Although a broadside radiation pattern is observed over the BW, higher cross-polar component is also present, as shown in Fig. 4(c). This higher cross polarization level will be advantageous in mobile and personal communication systems.

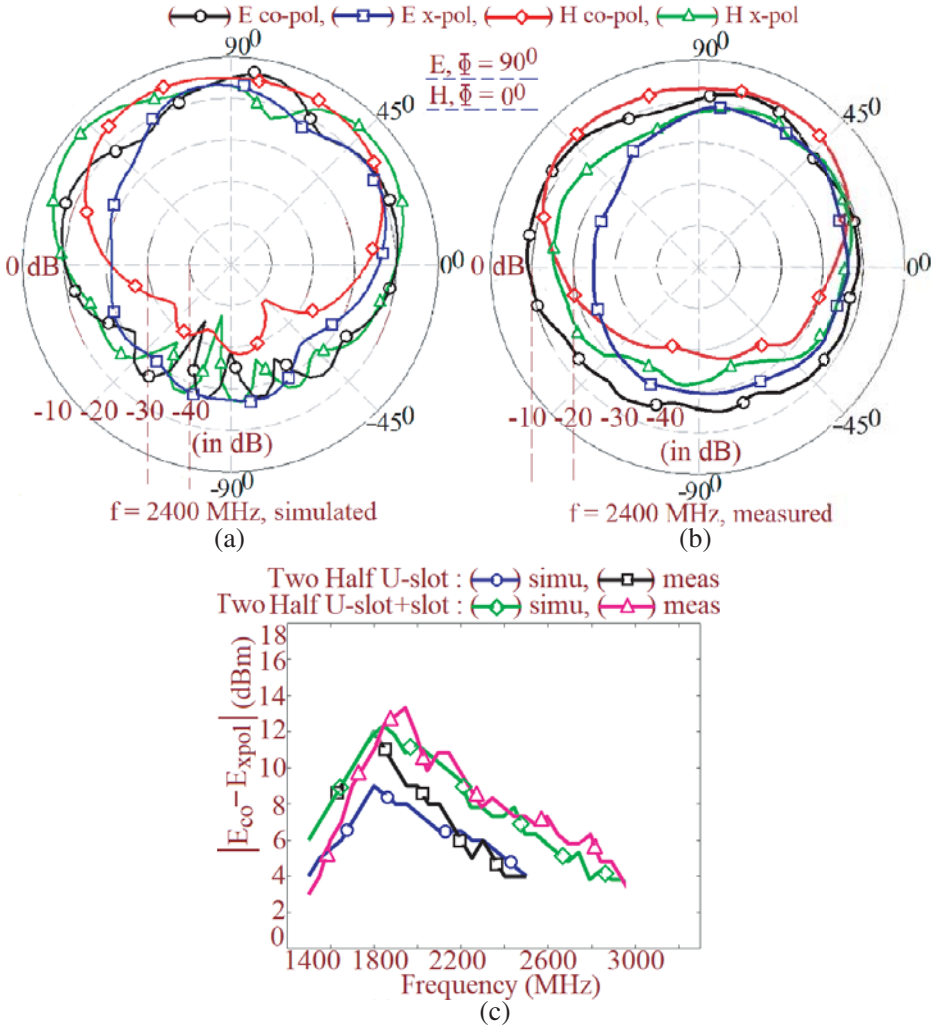

Figure 4. (a), (b) Radiation pattern nearer to band stop frequency for SMSA with two half U-slots and (c) cross polar level variation over the BW in broadside direction for SMSA with two half U-slots and a rectangular slot.

As observed from Fig. 2(d), the next resonant mode present in two half U-slot cut design is TM_{02}. Further increase in the BW is obtained by tuning this frequency with respect to modified TM_{11} and TM_{20} modes. To decide the additional rectangular slot position, the surface current distribution at modified TM_{02} mode is studied. Near the maxima of its surface currents, a rectangular slot of dimension

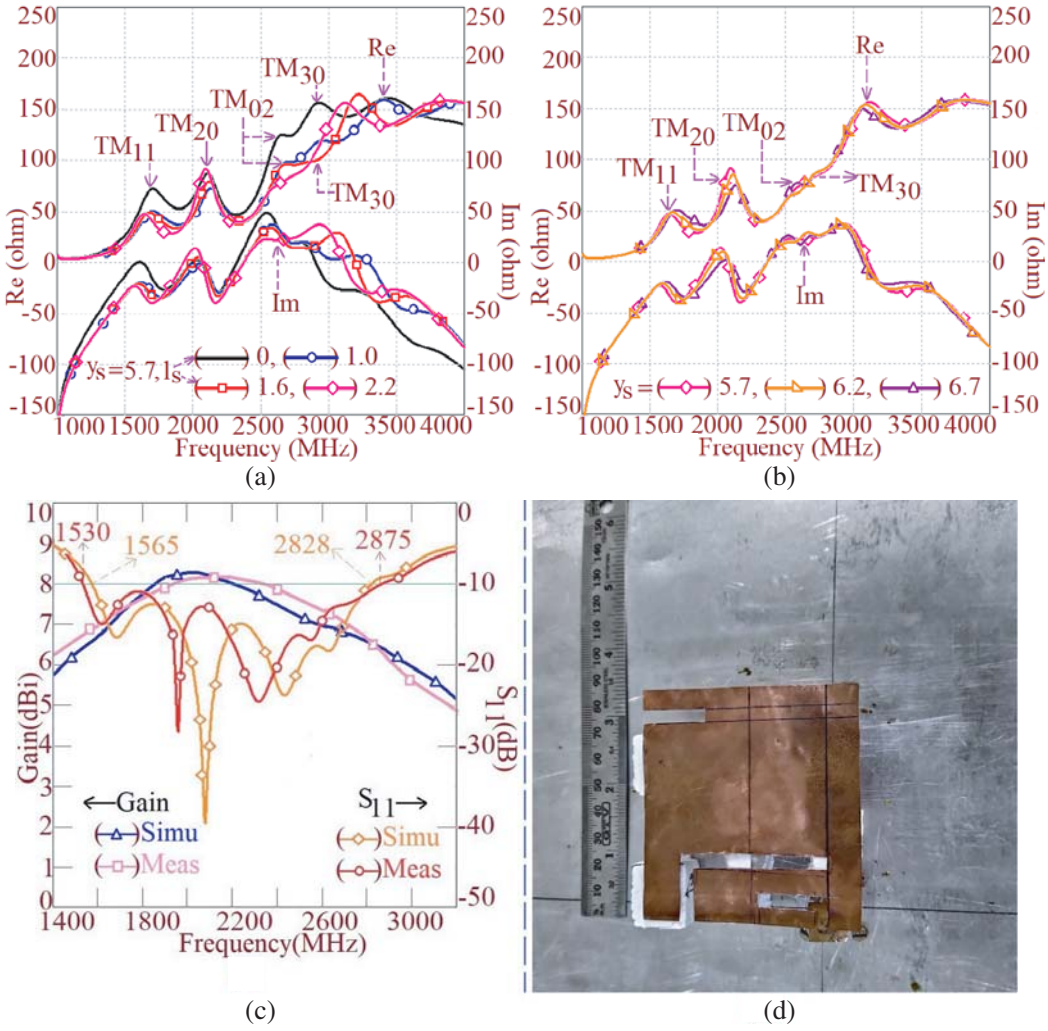

Figure 5. Resonance curve plots for variation in (a) L_s and (b) y_s, (c) return loss plots and (d) fabricated antenna for a rectangular slot cut two half U-slots cut nearly SMSA.

'$L_s \times w_{s1} \times y_s$' is cut as shown in Fig. 1(c). For 'w_{s1}' = 0.4 cm, parametric study is carried out for variation in slot dimensions, and resonance curve plots for them are shown in Figs. 5(a) and (b). With the increase in slot length, the frequency of TM_{02} mode decreases. Because of the circulation of surface currents around the slot edge, the frequency of TM_{30} mode also decreases. The slot position 'y_s' optimizes the impedance at TM_{02} and TM_{30} modes to give wide band response as shown in Fig. 5(c). The simulated and measured BWs using an additional rectangular slot are 1263 MHz (57.5%) and 1345 MHz (61%), respectively. The variations in the simulated and measured results are attributed to the errors in maintaining desired air gap for patch and proximity feeding strip. The antenna gain is more than 5 dBi over the complete BW with the peak value of 9 dBi. This antenna also shows a radiation pattern with higher cross polar levels across the BW as shown in Fig. 4(c). The fabricated antenna prototype is shown in Fig. 5(d). For the testing purpose antenna was fabricated using copper plate and supported in air using foam spacers. The radiation pattern and gain measurement setup is shown in Fig. 6. A distance of more than '$2D^2/\lambda$' is kept in between the reference antenna and the antenna under test. A wideband horn antenna is used as the reference antenna. Measurement was carried out inside an antenna lab, wherein minimum reflections from the surrounding objects were ensured at the measurement frequency. Also, the surrounding objects were non-metallic in nature, which minimizes reflections and yields closer agreement between the simulated and measured results.

Thus as against reported slot cut variations, the proposed antennas realizes a higher cross-polar

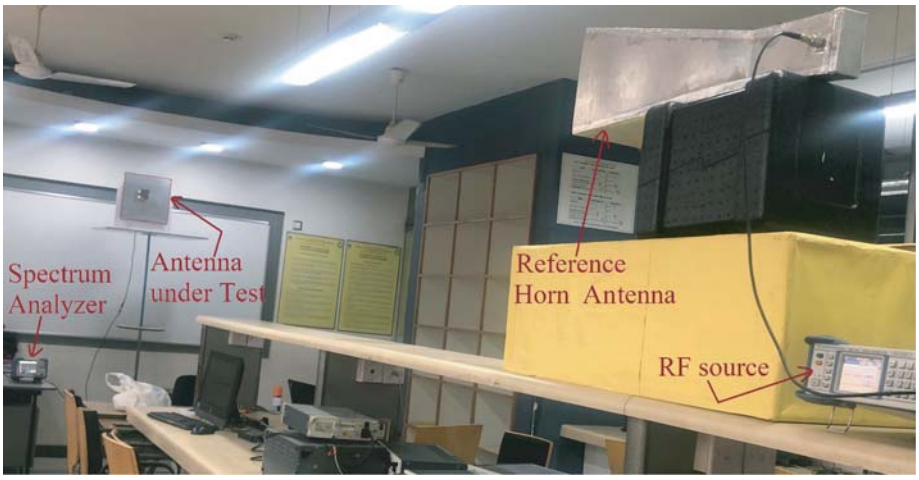

Figure 6. Measurement setup for a rectangular slot cut two half U-slots cut nearly SMSA.

pattern, as only higher order modes are present as against the fundamental modes. Hence, they will find applications in mobile and personal communication systems. Further formulation in resonant length for various modes present in the slot cut patch and subsequent design methodology is discussed.

3. RESONANT LENGTH FORMULATION AND DESIGN METHODOLOGY FOR TWO HALF U-SLOTS AND A RECTANGULAR SLOT CUT SMSA

The wideband response in the above multiple slots cut SMSA is realized due to the optimum spacing in between TM_{11}, TM_{20}, and TM_{02} mode frequencies with respect to TM_{10} and TM_{01} modes. Hence first the resonant length formulations at all these modes are proposed. For the same, at each modified patch mode, surface current distributions were studied extensively for different slot dimensions so as to arrive at the final resonant length equation. The resonant length formulations at various modes are given in Eqs. (1)–(4). In each equation, effects of individual slot lengths (i.e., 'L_{v1}', 'L_{u1}', 'L_{v2}', 'L_{u2}' and 'L_s') on respective resonant modes are added separately using respective terms. Each term for a particular slot length variation is selected by observing the variation in simulated frequencies and current vector directions against the slot length. Resonance length at TM_{11} mode is calculated by using effective patch length (L_e) and width (w_e) as calculated for the TM_{10} and TM_{01} resonant modes. The frequency at all the modes is calculated using Equation (5), and the % error between the simulated and calculated frequency is calculated using Equation (6). The plots of the two frequencies at each mode and % error in between them against the total slot length variation are shown in Figs. 7 and 8. Since each half U-slot and rectangular slot affects all the modes, the plots have been shown against the total slot length, i.e., $L_t = L_{v1}+L_{u1}+L_{v2}+L_{u2}+L_s$. As observed, closer prediction between two frequencies with % error less than 5% is obtained at each mode. Further using the proposed formulation, the design methodology to realize a similar multiple slots cut antenna at given frequency is explained. It is observed from the above study that band start frequency in multiple slots cut SMSA is close to 1500 MHz. The simulated TM_{10} mode frequency for the above equivalent SMSA is 1468 MHz, which is near the band start frequency.

At f_{10} mode

$$L_e = L + 2(0.65h) + (2L_{v1})\left(\frac{L_{v1}}{1.5W}\right)\cos\left(\frac{\pi x}{L}\right) + (2L_{u1})\left(\frac{L_{u1}}{1.2L}\right) + L_{v2}\left(\frac{L_{v2}}{W}\right)\cos\left(\frac{\pi x_1}{L}\right) + \frac{L_{u2}}{2L} + \frac{l_s}{L} \quad (1)$$

At f_{01} mode

$$\begin{aligned} W_e \;=\; & W + 1.25h + \frac{w_s}{4} + 0.116\,(2L_{u1})\left(\frac{L_{u1}}{L}\right)\cos\left(\frac{\pi y}{W}\right) + \frac{w_s}{4} \\ & + 0.25\,(2L_{u2})\left(\frac{L_{u2}}{L}\right)\cos\left(\frac{\pi y_1}{W}\right) + \left(\frac{l_s}{L}\right)\cos\left(\frac{\pi y_x}{W}\right) \end{aligned} \quad (2)$$

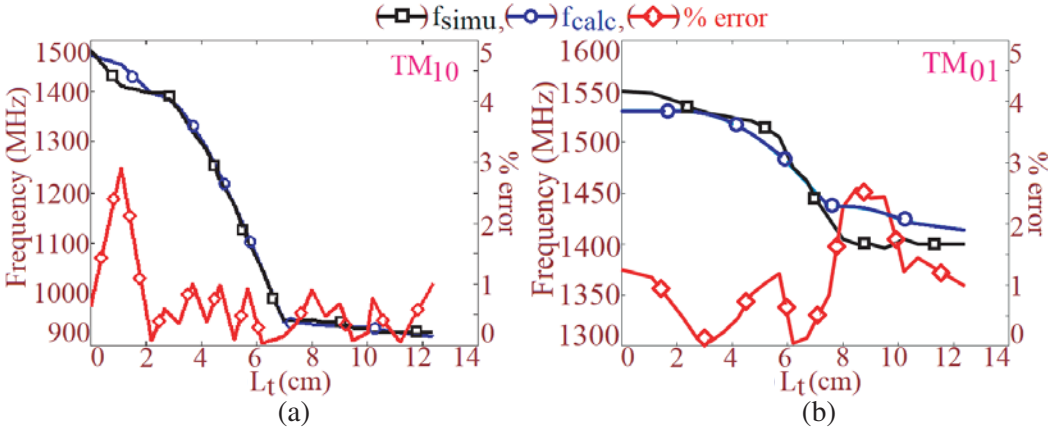

Figure 7. Frequencies and % error plots at (a) TM_{10} and (b) TM_{01} for a rectangular slot cut two half U-slots cut SMSA.

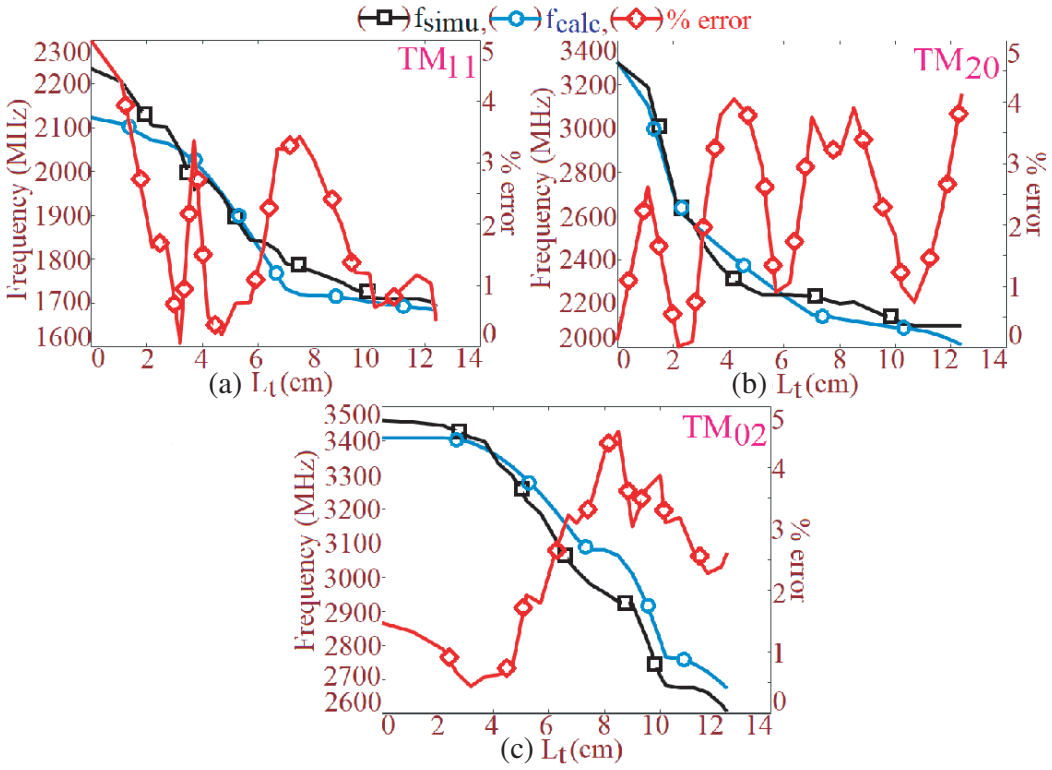

Figure 8. Frequencies and % error plots at (a) TM_{11} (b) TM_{20} and (b) TM_{02} modes for a rectangular slot cut two half U-slots cut SMSA.

At f_{20} mode

$$L_e = L + 0.74h + (2L_{v1})\left(\frac{L_{v1}}{0.56W}\right)\sin\left(\frac{2\pi x}{L}\right) + \left(\frac{L_{u1}}{0.25L}\right) + (2L_{v2})\left(\frac{L_{v2}}{2W}\right)\sin\left(\frac{2\pi x_1}{L}\right) + \frac{L_{u2}}{L} + (l_s)\left(\frac{l_s}{L}\right)\sin\left(\frac{2\pi y_x}{W}\right) \quad (3)$$

At f_{02} mode

$$W_e = W + 0.75h + \frac{w_s}{4} + 0.14\,(2L_{u1})\left(\frac{L_{u1}}{L}\right)\sin\left(\frac{2\pi y}{W}\right) + \frac{w_s}{4} + 2.7L_{u2}\left(\frac{L_{u2}}{L}\right)\sin\left(\frac{2\pi y_1}{W}\right) + (0.6l_s)\left(\frac{l_s}{L}\right)\sin\left(\frac{\pi y_x}{W}\right) \quad (4)$$

$$f_{11} = \frac{C}{2\sqrt{\varepsilon}_{eff}}\sqrt{\left(\frac{m}{L_e}\right)^2 + \left(\frac{n}{W_e}\right)^2} \quad (5)$$

$$\%\,\text{error} = \left|\frac{f_{calc} - f_{simu}}{f_{simu}}\right| \times 100 \quad (6)$$

Thus in the redesigning procedure for initial calculations, band start frequency of the desired BW is taken equal to TM_{10} mode frequency of SMSA. Hence, first SMSA length is calculated for the given f_{TM10} mode frequency. To yield larger BW, the design is presented on a substrate with the total thickness of $0.1\lambda_g$. Using Equation (7), SMSA length is calculated. For air substrate, dielectric constant is taken equal to unity whereas for suspended dielectric substrate, effective dielectric constant is calculated using Equation (8).

$$L = \left(\frac{30}{2f_{\text{TM10}}\sqrt{\varepsilon}_{re}}\right) - 2\left(\frac{0.65h_t}{\sqrt{\varepsilon}_{re}}\right) \quad (7)$$

$$\varepsilon_{re} = \frac{\varepsilon_r\,(h_a + h)}{\varepsilon_r h_a + h} \quad (8)$$

where $\varepsilon_{re} = 1$ for air substrate; ε_r is the dielectric constant of suspended substrate; 'h_t' is the total substrate thickness that equals '$h_a + h$' for suspended dielectric; 'f_{TM10}' is in GHz when 'L' is calculated in cm.

To realize closely spaced orthogonal modes, nearly square patch is selected, and thus W is taken equal to 0.95 L. A square proximity strip of length $0.06\lambda_g$ is placed at a thickness of $0.088\lambda_g$ below the patch and at a distance of $0.1224\lambda_g$ from the patch center. These parameters are selected based upon their values in the above optimum design, normalized with respect to the substrate TM_{10} mode wavelength (λ_g). Further inside this SMSA, two half U-slots of dimensions 'L_{v1}', 'L_{u1}', 'L_{v2}', and 'L_{u2}' and a rectangular slot of length 'L_s' are cut. Apart from these slot dimensions, parameters like slot width and slot positions from the patch edge also affect the variations in various modal frequencies. However, the trend in the variation of modal frequencies is largely governed by the slot lengths. Hence, slot width (w_s, w_{s1}) in all the cases is taken equal to $0.02\lambda_g$, whereas vertical lengths in two half U-slots are cut at a distance of $0.108\lambda_g$ ('x' and 'x_1' as mentioned in Fig. 1(c)) from the patch center. The rectangular slot is cut at a distance of $0.328\lambda_g$ from the patch edge as shown in Fig. 1(c). In each half U-slot, two slot dimensions namely 'L_v' and 'L_u' are present. It is observed in the parametric study that length 'L_v' mainly affects the impedance at various modes, whereas 'L_u' has more effect on the frequency. As the optimum response is a result of optimum spacing between frequencies followed by the impedance optimization, lengths 'L_{v1}' and 'L_{v2}' are selected as $0.108\lambda_g$ and $0.049\lambda_g$, respectively. These slot parameter values are again selected based upon their optimum values in the design at 2000 MHz as mentioned above. Further using Equations (1) to (5), against increasing 'L_{u1}', 'L_{u2}', and 'L_s', modified TM_{01}, TM_{10}, TM_{11}, TM_{20}, and TM_{02} mode frequencies are calculated. In single half U-slot patch, wideband response is the result of optimum spacing between TM_{11} and TM_{10} mode frequencies, and for this frequency ratio '$f_{\text{TM11}}/f_{\text{TM10}}$' of around 1.86 exists. Using the second half U-slot, which optimizes the frequency and impedance at TM_{20} mode, the ratio '$f_{\text{TM11}}/f_{\text{TM10}}$' is reduced to around 1.85, whereas using the rectangular slot TM_{02} mode frequency is optimized which gives a ratio around 3 with respect to TM_{10} mode. Using these frequency ratios, the redesign of slot cut configurations is presented for $f_{\text{TM10}} = 900$ MHz on an air substrate and 1200 MHz on a suspended FR4 substrate ($\varepsilon_r = 4.3$, $h = 0.16$ cm). Various antenna parameters and the frequencies of all the modified resonant modes against increasing slot lengths are calculated using above equations and formulations The calculated frequency ratio plots for f_{TM11} and f_{TM02} modes against f_{TM10} mode are shown in Figs. 9(a) and (b).

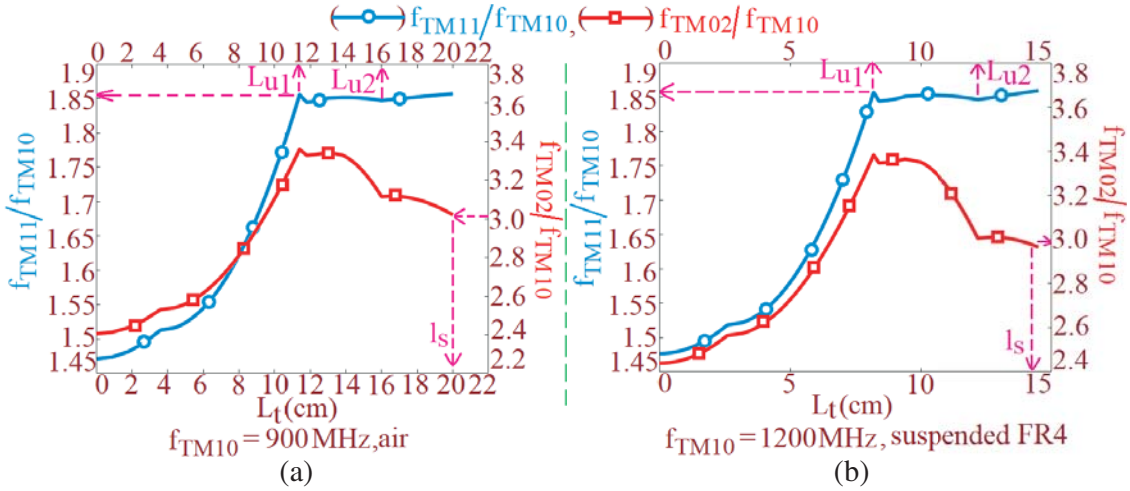

Figure 9. Frequency ratio plots among TM_{02}, TM_{11} and TM_{10} modes for two U-slots and rectangular slots cut SMSA for (a) air and (b) suspended FR4 substrate.

A value of total slot length 'L_t' is noted for which f_{TM11}/f_{TM10} is around 1.86. This will give $L_{u1} = L_t - L_{v1}$. Using these dimensions, first larger half U-slot is cut inside the SMSA. Further, a value of 'L_t' is noted for frequency ratio around 1.85. As seen from the plot, two values of 'L_t' exist. However, the first value is ignored, and the second one is selected. This value of 'L_t' will give $L_{u2} = L_t - L_{v1} - L_{u1} - L_{v2}$. Using these dimensions, a two half U-slots cut SMSA was designed and fabricated. Various design parameters for the two antennas are given in Table 1. The return loss plots for the antennas at 900 and 1200 MHz are shown in Figs. 10(a) and (b), respectively. The simulated and measured BWs at 900 MHz are 604 MHz (48.8%) and 632 MHz (51.5%), respectively. At 1200 MHz, these two values are 635 MHz (45.9%) and 686 MHz (49.53%), respectively. The variation in two BWs is attributed to experimental errors in maintaining the exact air gap for the patch and proximity strip. In the two cases, the BW lies near the f_{TM10} mode frequency of SMSA. Inside this two half U-slot cut

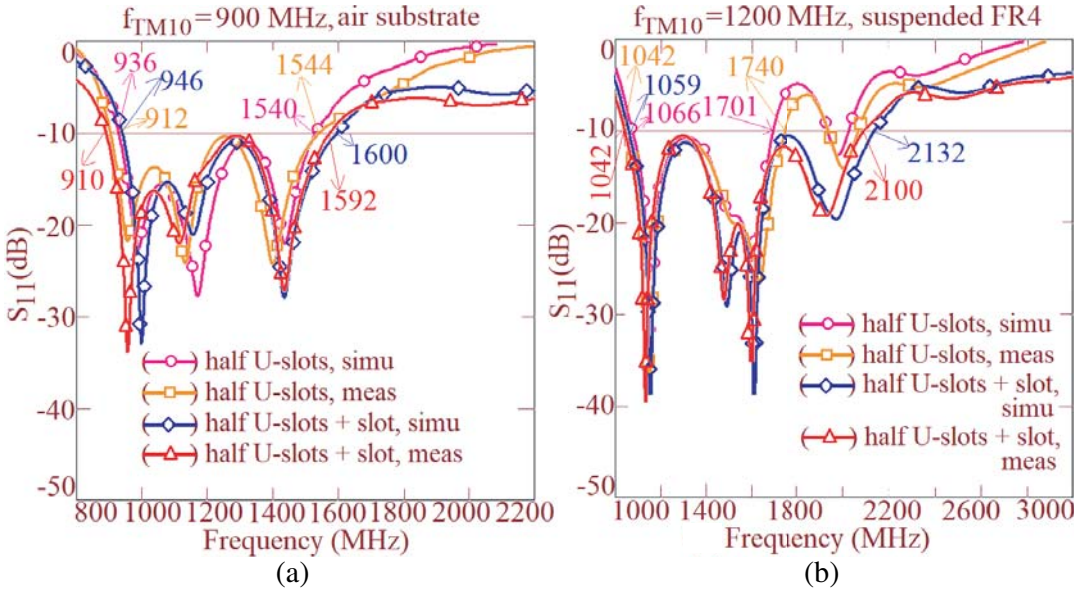

Figure 10. Return loss plots for two U-slots and rectangular slots cut SMSAs for (a) air and (b) suspended FR4 substrate.

Table 1. Various antenna parameters for the re-designed configurations.

f_{TM10}. substrate	900 MHz, air	2000 MHz, air	1200 MHz, FR4 suspended	2200 MHz, FR4 suspended
L, W (cm)	12.4, 11.8	5.6, 5.3	8.9, 8.4	4.6, 4.3
h, h_s, x_f (cm)	3.3, 2.9, 4.1	1.5, 1.3, 1.8	2.56, 2.2, 3.0	1.36, 1.1, 1.55
w_s (cm)	0.6	0.3	0.5	0.2
L_{v1}, L_{u1} (cm)	3.6, 7.8	1.6, 3.0	2.6, 5.6	1.4, 2.9
L_{v2}, L_{u2} (cm)	1.6, 3.2	0.7, 1.2	1.2, 2.8	0.6, 1.6
L_s, y_s (cm)	4.0, 10.9	1.8, 4.9	2.3, 7.8	1.0, 4.0
x, x_1 (cm)	3.6	1.6	2.6	1.4

Table 2. Comparison for proposed slot cut SMSA variations against reported slot cut designs.

MSA shown in	Meas. BW (MHz, %)	Peak Gain (dBi)	Cross polar level	Patch area	Substrate thickness
SMSA with two half U-slots	1022, 51.6	8.6	-7 dB	$3.6\lambda_c$	$0.13\lambda_c$
SMSA with two half U-slots + rectangular slot	1345 61	8.1	-7 dB	$4.02\lambda_c$	$0.134\lambda_c$
Ref [1]	470, 44.9	10	< -20 dB	$9.54\lambda_c$	$0.08\lambda_c$
Ref [2]	408, 24.82	7.2	< -25 dB	$3.74\lambda_c$	$0.076\lambda_c$
Ref [4]	1450, 21.49	8.5	-15 dB	$1.5\lambda_c$	$0.1\lambda_c$
Ref [5]	3000, 53.6	10.2	< -12 dB	$2.1\lambda_c$	$0.124\lambda_c$
Ref [6]	580, 27.62	9.41	—	$2.93\lambda_c$	$0.101\lambda_c$
Ref [7]	80, 9.3	7	-22 dB	$5.28\lambda_c$	$0.043\lambda_c$
Ref [9]	590, 53.9	8	-10 dB	$7.11\lambda_c$	$0.104\lambda_c$
Ref [10]	700, 31	8.5	-7 dB	$1.672\lambda_c$	$0.07\lambda_c$
Ref [11]	2020, 68	10	-34 dB	$2.244\lambda_c$	$0.02\lambda_c$
Ref [14]	700, 44	9.9	< -20 dB	$5.975\lambda_c$	$0.09\lambda_c$
Ref [15]	351, 6.6	6.5	-25 dB	$0.28\lambda_c$	$0.083\lambda_c$
Ref [17]	45%	8.5	-16 dB	$35\lambda_c$	$0.076\lambda_c$
Ref [18]	74, 3.93	1.0	-7 dB	$2.12\lambda_c$	$0.021\lambda_c$
Ref [19]	1150, 21	10	-24 dB	$1.378\lambda_c$	$0.036\lambda_c$

SMSA, a rectangular slot 'L_s' is cut. For this value of 'L_t' is noted for which '$f_{\text{TM02}}/f_{\text{TM10}}$' ratio is around 3. Using this value of 'L_t' slot length is calculated as $L_s = L_t - L_{v1} - L_{u1} - L_{v2} - L_{u2}$. For this length, antenna is simulated, and fabrication was done for the measurement purpose. The results with an additional slot at 900 and 1200 MHz are shown in Figs. 10(a) and (b).

The simulated and measured BWs at 900 MHz are 654 MHz (51.3%) and 682 MHz (54.52%), respectively. At 1200 MHz, these two values are 1073 MHz (67%) and 1058 MHz (67.34%), respectively. Smaller increment in BW for the design at 900 MHz than two half U-slot configuration is attributed to the reduced coupling to the modified TM_{02} mode on the air substrate. Antennas were also designed at other frequencies as mentioned in Table 1. They show a similar wideband response. Thus, the proposed methodology is useful in the design of wideband multiple slots cut nearly square patch antennas near

given band start frequency, on the thicker substrate. The comparison for the proposed multiple slots cut antenna with some of the reported designs is provided in Table 2. The patch area and substrate thickness as mentioned in Table 2 are normalized with respect to the guided wavelength (λ_c) at the center frequency of BW. Also the cross-polar level as mentioned in Table 2 is noted at the center frequency of the BW.

The initial designs of slot cut MSAs [1, 2], or modified slot cut patch variations [4, 19], or slot cut designs on a thinner substrate than $0.04\lambda_0$ [7], or the offset slot cut and multiple slots cut antennas [5, 6, 9, 10, 14, 18] were optimized with reference to the fundamental mode. Hence, they offer either lower cross-polar radiation throughout the BW or larger cross-polar radiation only across certain range of frequencies over the BW. As against that proposed configurations offer larger cross-polar radiation over the entire BW and give higher VSWR BW with comparable values of other antenna parameters. A large impedance BW on lower substrate thickness was obtained in the two U-slot cut antenna design reported in [11]. But it requires differential feeding, and the reported work does not clearly explain which modes contribute towards the pattern reconfiguration as well as the effects of substrate thickness on impedance matching at respective modes. Further in frequency reconfigurable designs using slots [15, 16], detailed theory about antenna functioning by highlighting the effects of U-slot along with diodes is not put forward. A similar study lacks in modified E-shape design as reported in [17]. In comparison, the present paper puts forward detailed theory about antenna functioning in terms of patch modes as well as proposes design methodology using resonant length formulations. Thus, designs of multiple slots cut antennas offering higher impedance BW around modified higher modes and showing higher cross polar radiation throughout the BW supported with design methodology are the new technical contributions in the proposed work against reported multiple slot cut designs offering wideband response.

4. CONCLUSIONS

Designs of multiple slots cut nearly SMSA using the combinations of half U-slots and a rectangular slot are proposed for the wideband response. As against the reported slot cut variations, the proposed designs offer wide band response around the higher order TM_{11}, TM_{20}, and TM_{02} mode frequencies, to give higher impedance BW along with a high cross-polar radiation pattern. The maximum BW of nearly 61% is obtained in the design using two half U-slots and a rectangular slot. The proposed antennas offer a broadside radiation pattern with higher cross-polar level and a broadside gain above 5 dBi across the entire BW. The resonant length formulations at modified patch modes and subsequent design methodology using the same are presented. This is useful in the redesigning of similar configurations at different resonance frequencies on thicker substrates. The proposed configurations will find applications in personal and mobile communication applications where signal loss due to polarization mismatch is to be minimized.

REFERENCES

1. Huynh, T. and K. F. Lee, "Single-layer single-patch wideband microstrip antenna," *Electronics Letters*, Vol. 31, No. 16, 1310–1312, 1995.
2. Wong, K. L. and W. H. Hsu, "A broadband rectangular patch antenna with a pair of wide slits," *IEEE Transactions on Antennas & Propagation*, Vol. 49, No. 9, 1345–1347, 2001.
3. Wong, K. L., *Compact and Broadband Microstrip Antennas*, 1st Edition, John Wiley & Sons, Inc., New York, USA, 2002.
4. Tiwari, R. N. P. Singh, and B. K. Kanaujia, "Butter fly shape compact microstrip antenna for wideband applications," *Progress In Electromagnetics Research*, Vol. 69, 45–50, 2017.
5. Sharma S. K. and L. Shafai, "Performance of a novel Ψ-shaped microstrip patch antenna with wide bandwidth," *IEEE Antennas Wireless Propagation Letters*, Vol. 8, 468–471, 2009
6. Islam, M. T., M. N. Shakib, and N. Misran, "Multi-slotted microstrip patch antenna for wireless communication," *Progress in Electromagnetic Research Letters*, Vol. 10, 11–18, 2009.

7. Chen, Y., S. Yang, and Z. Nie, "Bandwidth enhancement method for low profile e-shaped microstrip patch antennas," *IEEE Transactions on Antennas & Propagation*, Vol. 58, No. 7, 2442–2447, 2010.
8. Bhardwaj, S. and Y. R. Samii, "A comparative Study of C-shaped, E-shaped, and U-slotted patch antennas," *Microwave and Optical Technology Letters*, Vol. 54, No. 7, 1746–1756, 2012.
9. Deshmukh, A. A., D. Singh, and K. P. Ray, "Modified designs of broadband e-shape microstrip antennas," *Sadhana — Academy Proceedings in Engineering Science*, 44–64, Springer Publication, 2019.
10. Khodaei, G. F., J. Nourinia, and C. Ghobadi, "A practical miniaturized u-slot patch antenna with enhanced bandwidth," *Progress in Electromagnetic Research B*, Vol. 3, 47–62, 2008.
11. Radavaram, S. and M. Pour, "Wideband radiation reconfigurable microstrip patch antenna loaded with two inverted U-slots," *IEEE Transactions on Antennas & Propagation*, Vol. 67, No. 3, 1501–1508, 2019.
12. Deshmukh A. A. and K. P. Ray, "Analysis of broadband variations of U-slot cut rectangular microstrip antennas," *IEEE Antennas and Propagation Magazine*, Vol. 57, No. 2, 181–193, 2015.
13. Deshmukh A. A., and K. P. Ray, "Analysis of broadband Ψ-shaped microstrip antennas," *IEEE Antennas Propagation Magazine*, Vol. 55, No. 2, 107–123, 2013.
14. Guo, Y. X., K. M. Luk, K. F. Lee, and Y. L. Chow, "Double U-slot rectangular patch antenna," *Electronics Letters*, Vol. 34, No. 19, 1805–1806, 1998.
15. Qin, P.-Y., Y. J. Guo, A. R. Weily, and C.-H. Liang, "A pattern reconfigurable U-slot antenna and its applications in MIMO systems," *IEEE Transactions on Antennas & Propagation*, Vol. 60, No. 2, 516–528, 2012.
16. Qin, P.-Y., A. R. Weily, Y. J. Guo, and C.-H. Liang, "Polarization reconfigurable U-slot patch antenna," *IEEE Transactions on Antennas & Propagation*, Vol. 58, No. 10, 3383–3388, 2010.
17. Yin, J., Q. Wu, C. Yu, H. Wang, and W. Hong, "Broadband symmetrical E-shape patch antenna with mode resonance for 5G millimeter wave applications," *IEEE Transactions on Antennas & Propagation*, Vol. 67, No. 7, 4474–4483, 2019.
18. Xiao, S., Z. Shao, B.-Z. Wang, M.-T. Zhou, and M. Fujise, "Design of low profile microstrip antenna with enhanced bandwidth and reduced size," *IEEE Transactions on Antennas & Propagation*, Vol. 54, No. 5, 1594–1599, 2006.
19. Ge, Y., K. P. Esselle, and T. S. Bird, "A compact E-shaped patch antenna with corrugated wings," *IEEE Transaction on Antennas & Propagation*, Vol. 54, No. 8, 2411–2413, 2006.
20. CST Microwave Studio suite, Version 2019.